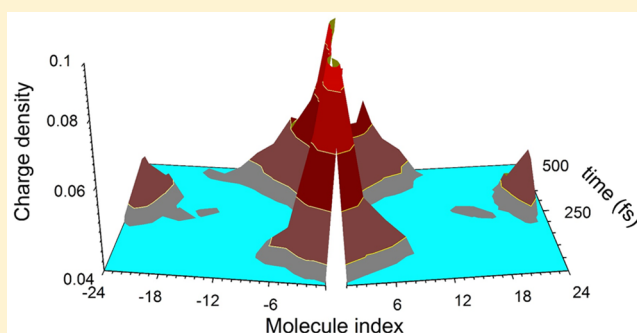


Ultrafast Long-Range Charge Separation in Organic Photovoltaics: Promotion by Off-Diagonal Vibronic Couplings and Entropy Increase

Yao Yao,[†] Xiaoyu Xie,[‡] and Haibo Ma^{*,‡}[†]Department of Physics, South China University of Technology, Guangzhou 510640, China[‡]Key Laboratory of Mesoscopic Chemistry of MOE, Collaborative Innovation Center of Chemistry for Life Sciences, School of Chemistry and Chemical Engineering, Nanjing University, Nanjing 210023, China**S** Supporting Information

ABSTRACT: The exciton dissociation in a model donor/acceptor heterojunction with electron–phonon couplings is simulated by a full quantum dynamical method, in which ultrafast long-range charge separation is observed. Such a novel scenario does not undergo short-range interfacial (pinned) charge transfer states, but can be mainly ascribed to the quantum resonance between local Frenkel excited states and a broad array of long-range charge transfer (LRCT) states assisted by the moderate off-diagonal vibronic couplings. The entropy-increasing effect associated with the very dense density of states for LRCT states is also found to be beneficial for lowering the free energy barrier for charge generation in organic solar cells.



One of the most significant experimental advances in recent studies of organic solar cells (OSCs) is the observation of ultrafast charge separation with an electron–hole (e–h) separation distance being at least 4 nm in an extraordinarily short time scale of 10^1 – 10^2 fs.^{1–9} Evidently comprehending the underlying mechanism is useful for the future rational design of new OSCs with improved efficiency, but unfortunately such novel phenomena cannot be explained by the traditional theories. The charge separation in OSCs is traditionally accounted to take place within a time scale of 10^1 – 10^2 ps and consist of four fundamental steps: (1) generation of local Frenkel excitons (FEs) upon photoexcitation; (2) diffusion of FEs to the electron donor/acceptor (D/A) interface; (3) charge transfer between neighboring D and A molecules; (4) charge diffusion and charge collection at the electrodes, although the mechanism of how electrons and holes escape from the strong Coulomb attraction at the D/A interface is still controversial.^{10–27} Investigating the ultrafast processes in organic condensed phase is even more challenging because, within a short subpicosecond time scale, not only the quantum effects of excitons but also those of phonons and electron–phonon (vibronic) interactions emerge and become considerable, and, therefore, one cannot study the processes as incoherent events. Under such circumstances, nonperturbative quantum dynamics analysis is necessary.

Recently there have been many insightful theoretical attempts to interpret the ultrafast charge separation in OSCs.^{28–34} For example, Tamura et al.²⁸ found that both the charge delocalization and the vibronic hot nature of charge transfer (CT) state promote subpicosecond charge separation

in oligothiophene/fullerene interfaces via multiconfiguration time-dependent Hartree dynamics simulation. The interplay between mixed domains, domain geometry, and exciton delocalization were also examined by Heitzer et al.²⁹ with a kinetic Monte Carlo model, and it was concluded that up to 40% of the ultrafast component can be explained by geometric factors alone. Smith and Chin^{31,32} further addressed the issue of hot electronic states and suggested that ultrafast charge separation in PCBM arises from its broad range of electronic eigenstates, and vibrational fluctuations enable their rapid transitions. So far, a comprehensive picture about ultrafast charge separation is still missing due to the technique challenges for its accurate simulation, especially the following three facts. First, high-level quantum dynamics simulation is not applicable for systems of aggregate size. Second, due to the many-body effect induced by long-range Coulomb attractions for e–h pairs, much more electronic states are involved in charge separation than in carrier diffusion, i.e., $N \times N$ CT states versus N electron (or hole) states in a model system consisting of N donor molecules and N acceptor ones. The high density of states (DOS) of long-range CT (LRCT) states at the D/A interface has been recently found to be essential for the resonance between LRCT and FE states.^{12,14,27,30,35–37} Last but not the least, different from carrier diffusion, charge separation is exothermic, and therefore the effect of off-diagonal vibronic couplings, the coupling between different diabatic electronic

Received: October 16, 2016

Accepted: November 11, 2016

Published: November 11, 2016

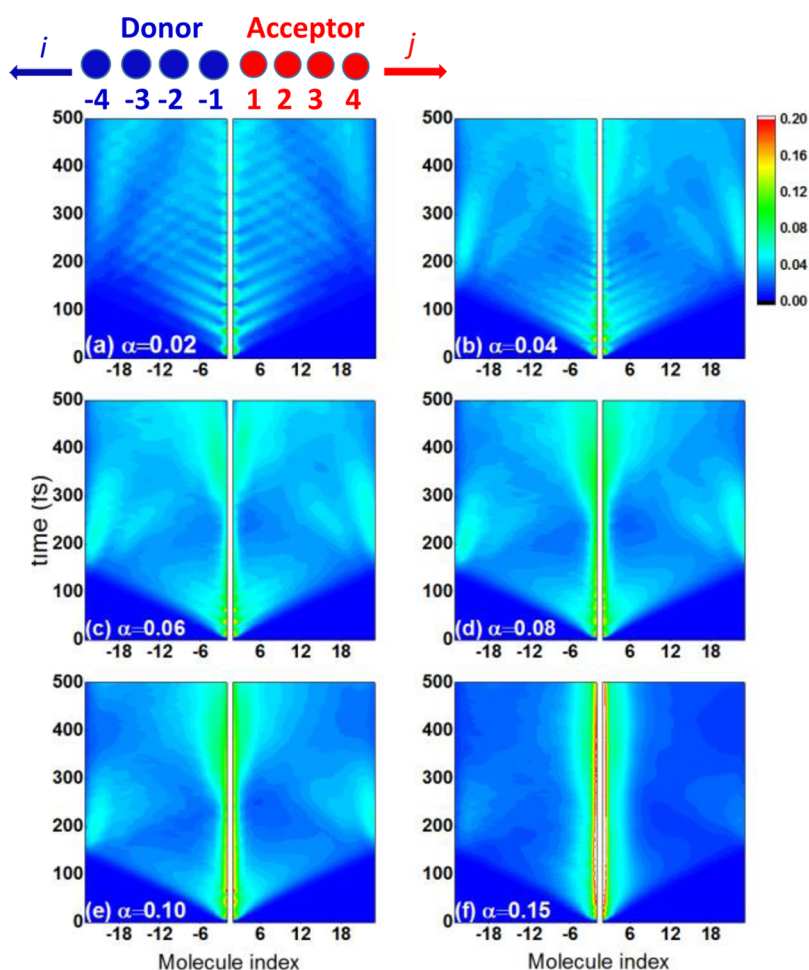


Figure 1. Charge density evolution of hole in the donor part and electron in the acceptor part with different α values.

states caused by the electron–phonon interactions, would play a much more important role in charge separation as recently indicated by Bittner and Silva.³⁰

How the free charges can be generated in OSCs is closely related to the transition between FE and LRCT states, in which short-range CT (SRCT) states are usually considered as intermediates to undergo. However, recent optical absorption simulations by one of us and his colleague¹⁴ as well as D’Avino et al.²⁷ revealed that FE and LRCT states can be energetically close, and, accordingly, LRCT states can be directly photo-excited upon hybridization with FE states via quantum resonance, which was verified by the latest experimental assignment of the full CT state absorption spectrum in microcrystalline rubrene/ C_{60} .³⁸ In another seminal work by Bittner and Silva,³⁰ it was proposed that resonant tunneling processes between them can be further enhanced by environmental fluctuations without undergoing SRCT states and produce charge separation on <100 fs time scales. Their transition rate was estimated at the Fermi golden rule (FGR) level, possibly not accurate enough for a quantitative evaluation of ultrafast processes with significant quantum vibronic effects. Moreover, a real-time quantum dynamics simulation would be highly desired to obtain the spatial-temporal evolution picture of ultrafast charge separation. To achieve this goal, for an exciton–phonon model at D/A interface, in this work we performed quantum dynamics simulations to present real-time dynamics of local FE, LRCT and SRCT states. Herein, we

removed the limitations in many previous models, by incorporating multiple instead of one donor site(s) to include all CT configurations, considering not only diagonal but also off-diagonal vibronic couplings, and simulating the real-time dynamics via a full quantum dynamics method, the time-dependent density matrix renormalization group (tDMRG) approach,^{20,39–41} instead of perturbative methods.

In our calculations, we simulate the charge separation dynamics from initial local FEs within a one-dimensional (1D) model chain (see top panel of Figure 1) consisting of N electron donor (D) molecules and N electron acceptor (A) molecules. Here we use a mixed Frenkel-CT-phonon model Hamiltonian as

$$H = H_{\text{ex}} + H_{\text{ph}} + H_{\text{ex-ph}} \quad (1)$$

Three contributions comprise the Hamiltonian: the exciton part, the phonon part, and the vibronic interaction. The first term H_{ex} has a form of

$$\begin{aligned} H_{\text{ex}} = & E_{\text{ex}}|-1\rangle\langle-1| - \sum_{i,j} \frac{c}{r_{i,j}}|i,j\rangle\langle i,j| \\ & + \sum_i \sum_{\{j,j'\}} V_A|i,j\rangle\langle i,j'| - \sum_j \sum_{\{i,i'\}} V_D|i,j\rangle\langle i',j| \\ & + V_{\text{DA}}|-1\rangle\langle-1,1| \end{aligned} \quad (2)$$

with $V_{\text{D/A/DA}}$ denoting the couplings between different electronic configurations ($|i\rangle$) for FE localized on site i and l

$i,j\rangle$ for a CT state with an electron transferred from a donor site i (<0) to an acceptor site j (>0). In addition, E_{ex} is the on-site energy for the FE configuration $|i\rangle$, C is the Coulomb energy between an electron and a hole at nearest-neighboring sites, and r_{ij} is the distance between site i and j . The symbol $\{i,i'\}$ or $\{j,j'\}$ indicates that the summation is limited to the nearest-neighboring sites. For concentrating on the illustration of the exciton dissociation dynamics at the D/A interface, here only one localized FE state $| -1\rangle$, which is closest to the D/A interface, is considered. Based on recent first-principles evaluations of electronic couplings in realistic tetracene/perylene-3,4,9,10-tetracarboxylic dianhydride (PTCDA) heterojunctions¹⁴ and the widely recognized exciton binding energy in OSCs,²⁶ here we took the typical parameter values of $E_{\text{ex}} = 0.25$ eV, $C = 0.48$ eV, $V_{\text{DA}} = 0.08$ eV, and $V_{\text{D}} = V_{\text{A}} = 0.06$ eV for D/A heterojunctions in OSCs.^{12,35–37}

The phonon part H_{ph} has an expression as

$$H_{\text{ph}} = \sum_{\nu} \omega_{-\nu} \hat{b}_{-\nu}^{\dagger} \hat{b}_{-\nu} + \sum_{\nu} \omega_{+\nu} \hat{b}_{+\nu}^{\dagger} \hat{b}_{+\nu} \quad (3)$$

where $\hat{b}_{-\nu}^{\dagger}$ (or $\hat{b}_{-\nu}$) is the creation (or annihilation) operator of the ν th oscillator mode localized on the donor ($-$) or acceptor ($+$) molecules, and $\omega_{\pm\nu}$ denotes the phonon frequency. For the exciton–phonon interactions, here we are mainly focusing on the effect of off-diagonal couplings, and the effect of diagonal vibronic couplings is found to be not relevant for the ultrafast long-range charge separation in Supporting Information. The off-diagonal vibronic couplings has the form

$$H_{\text{ex-ph}} = \sum_{i,j,\nu} \gamma_{-\nu} [|i, j\rangle \langle i-1, j | \hat{b}_{-\nu}^{\dagger} + |i-1, j\rangle \langle i, j | \hat{b}_{-\nu}] \\ + \sum_{i,j,\nu} \gamma_{+\nu} [|i, j\rangle \langle i, j+1 | \hat{b}_{+\nu}^{\dagger} + |i, j+1\rangle \langle i, j | \hat{b}_{+\nu}] \quad (4)$$

where $\gamma_{\pm\nu}$ is the coupling strength for ν th mode in donor ($-$) and acceptor ($+$) respectively, dependent on the spectral density $J(\omega)$. A continuous spectral density $J(\omega) = 2\pi\alpha\omega_c^{1-s}\omega^s e^{-\omega/\omega_c}$ is assigned for the phonon baths where α is the dimensionless coupling, s being the exponent. ω_c is the cutoff frequency, taken to be 2 eV, sufficiently large to converge the results. In this work, s is fixed to be 0.5 as in the other works^{41,42} for OSCs. For mimicking the dynamics in a full quantum manner, the tDMRG algorithm was employed. More methodology details can be found in the Supporting Information.

To model the exciton dissociation, the initial population localized on the FE state at the D/A interface ($| -1\rangle \langle -1 |$) is used in all our simulations, and then we study the population evolution from local FE state to CT states under different vibronic coupling strengths (α). In Figure 1, we illustrate the hole (electron) density evolution at the individual molecules. Clearly the effect of vibronic couplings on charge separation is not monotonic. For small $\alpha = 0.02$, following time evolving, the wavepacket of the charge density splits into two, which spread to the respective ends gradually and respectively until being bounced back after reaching the boundaries. This process can be well identified in traditional theories as charge transfer at the nearest D/A interface and the subsequent charge diffusion site by site.

Interestingly, an ultrafast long-range charge separation scenario is observed for moderate off-diagonal vibronic

couplings. When $0.04 \leq \alpha < 0.15$, at molecules -24 to -20 and 20 – 24 , the hole and electron states are found to be heavily populated between 150 and 350 fs. Because these high charge densities emerge far away from the interface in such a short time scale instead of being derived from the intermediate SRCT states, this implies a long-range charge separation mechanism. Such a new scenario is in agreement with Bittner and Silva's recent proposed mechanism of direct coupling between photoexcitations and photocurrent by FGR calculation³⁰ and can be ascribed to the quantum resonance between the energetically close FE and LRCT states,^{14,27,30} which will be examined later. Moreover, one may also notice that the further increased vibronic coupling strength ($\alpha \geq 0.15$) is not beneficial to charge separation. For the purpose of ruling out the other possible reasons on long-range charge separation, we also performed comparative simulations and found that our findings are independent of the system size and long-range charge separation is not obvious in the presence of only diagonal vibronic couplings (see Supporting Information).

To understand how off-diagonal vibronic couplings affect the charge separation, we consider their broadening effect on the DOS, as sketched in Figure 2a. The detailed calculated data are

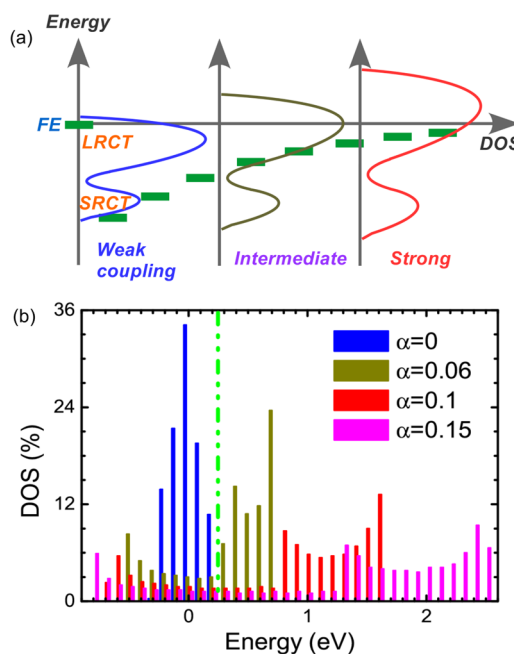


Figure 2. (a) Schematic CT DOS for weak, intermediate, and strong vibronic couplings. The diabatic CT states are sketched by green dashes. (b) The calculated CT DOS for four coupling strengths. The green dash-dot-dot line denotes FE energy.

shown in Figure 2b. It is obvious that the CT DOS with zero off-diagonal vibronic coupling ($\alpha = 0$) spreads over the energy range between -0.5 and 0.2 eV with very small energetic overlap with local FE states around 0.25 eV, where low energy states usually correspond to SRCT states with strong Coulomb attractions and high energy states correspond to LRCT ones with weak Coulomb attractions. Contributed by the coherence induced energy splitting, the energy distribution of CT DOS becomes broadened with the increasing off-diagonal vibronic coupling. For $\alpha = 0.06$, the CT DOS is distributed around FE energy of 0.25 eV in a balanced way, paving the way for the ultrafast charge separation via quantum resonance by effective

energetic overlaps between local FE and CT states. However, further increasing α makes DOS more dispersed and push the main peaks far beyond the energy of FE, weakening the resonance of FE and LRCT states. Therefore, the increasing magnitude of off-diagonal vibronic coupling has a non-monotonic effect on the efficiency of ultrafast long-range charge separation, for which an intermediate value of such couplings may give rise to the optimal performance.

To have a more intuitive picture on the charge separation dynamics, in the following we will show the temporal evolution of the e–h distance. On the basis of the population of electron and hole, we calculate the effective centers of the hole and electron wavepackets, respectively, which are defined as

$$i_{\text{hc}}(t) = \sum_{i < 0} i \rho_i(t), j_{\text{ec}}(t) = \sum_{j > 0} j \rho_j(t) \quad (5)$$

where $\rho_{i(j)}(t)$ is the hole (electron) density at site $i(j)$. Based on these two quantities, it is straightforward to define the e–h distance as $d_{\text{e-h}} = j_{\text{ec}} - i_{\text{hc}}$. In Figure 3a, the time evolution of

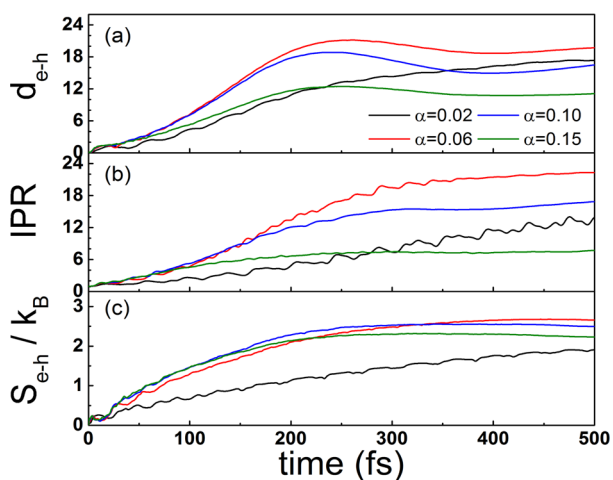


Figure 3. Evolution of (a) e–h distance ($d_{\text{e-h}}$), (b) IPR, and (c) total e–h entropy ($S_{\text{e-h}}$) for four α 's.

$d_{\text{e-h}}$ is shown for four α 's. For weak coupling case ($\alpha = 0.02$), $d_{\text{e-h}}$ continues increasing within $t < 500$ fs, implying that there is no ultrafast long-range charge separation, and the electron and hole separate only via charge diffusion from site to site. For $\alpha > 0.02$ cases, $d_{\text{e-h}}$ increases rapidly and reaches its maximum around 250 fs. $\alpha = 0.06$ gives the longest $d_{\text{e-h}}$ among all the coupling cases, which closely equals half of the system size (24 molecules) of our model system. The rapid growth and saturation of $d_{\text{e-h}}$ are expected to be contributed by the quantum resonance between local FE and LRCT states.

Recent investigations^{14,27} evidenced that the resonance between FE and LRCT states is usually accompanied by the charge delocalization over tens of molecules. As, in our present model, both the electronic couplings and vibronic couplings are concurrently involved, one may argue that the nonlocal e–h coherence may arise from the spatial delocalization of the electron/hole wave function assisted by the electronic couplings among different molecules instead of the quantum resonance promoted by off-diagonal vibronic couplings. In Figure 3b, we show the inverse participation ratio (IPR) defined by $\text{IPR} = 1/\sum_i \rho_i^2$ to measure the wave function delocalization. Following time evolving, IPR slightly lags behind $d_{\text{e-h}}$, that is, the IPR persists to be smaller than $d_{\text{e-h}}$

reaches its maximum. It implies that, the long-range separation between the electron and the hole occurs well before their wavepackets spread, which makes the IPR increase. Indeed, the LRCT state is initially quite localized as shown in Figure 1, which means the initial nonlocal coherence is essentially induced by the off-diagonal vibronic couplings instead of the electronic couplings.

To characterize the entropy change during the charge separation, we calculated the entropy by the electronic contribution defined by $S = -k_B \text{Tr} \rho \ln \rho$ and displayed its time evolution in Figure 3c. It is evident that entropy increases with time evolving, where the weak vibronic coupling gives the slowest increasing. It should be noted that, the increase of entropy, induced by the DOS of LRCT states much larger than that of SRCT ones,^{12,14,35,36} is associated with the decrease of the free energy $F(\equiv E - TS)$. From Figure 3c it is found that, the largest entropy increase for $\alpha = 0.06$ is about 2.7 k_B . At room temperature, this corresponds to 70 meV decrease of the free energy barrier. In realistic three-dimensional D/A interfaces, the entropy increase will be approximately three times as large as in our 1D model,⁴³ and, accordingly, the free energy barrier for exciton dissociation can be reduced by 0.21 eV, considerably large for efficient charge separation and close to Hood and Kassal's recent estimation.⁴⁴ In all, our results indicated that the recently addressed importance of entropy^{11,18,44} also exists in long-range charge separation in OSCs.

Before the end, two issues should be mentioned. First, the ground state of phonons is assigned as the initial state of the time evolution. For considering the temperature effect, we applied the heating operators to the initial phonon states, and our results of $d_{\text{e-h}}$ and IPR do not exhibit significant differences between cases with or without heating process (see Supporting Information for details). The reason is 2-fold. The binding energy of the shortest-range CT state is around 0.48 eV, much larger than the thermal energy at room temperature, and the time scale of ultrafast charge separation is much shorter than the featured time scale of thermal fluctuation. It is thus safe to conclude that the temperature effect will not alter the nature of the ultrafast charge separation process observed here. Second, one should also notice that the ultrafast long-range charge separation revealed in our tDMRG simulation cannot be observed by traditional perturbative methods. In our simulations by Redfield theory, a typical perturbative quantum dynamics method, only short-range charge diffusion site by site was observed (see Supporting Information). It is not unexpected because the broadening of LRCT DOS, which is crucial for long-range charge separation, cannot be triggered by Redfield theory. The perturbation treatment of vibronic couplings can only destroy the quantum coherence between electronic configurations via dissipation, leading to short-range charge diffusion, which is significantly slower than long-range charge separation via quantum resonance and cannot explain the subpicosecond ultrafast charge separation observed in experiments. This enlightens the necessity of using full quantum dynamics methods for simulating ultrafast processes in OSCs.

In conclusion, we examined the effects of vibronic couplings on exciton dissociation dynamics in OSCs through a full quantum dynamics simulation within a 1D D/A heterojunction model. Specifically, we observed long-range charge separation in an ultrafast time scale of < 350 fs. Detailed analysis indicated that it is caused by the quantum resonance between local FE states and a broad array of LRCT states assisted by the

moderate off-diagonal vibronic couplings. Such transitions from FE to LRCT states in association with the increasing e–h entropy can be considered as the driving force for ultrafast charge separation in OSCs.

■ ASSOCIATED CONTENT

Supporting Information

The Supporting Information is available free of charge on the ACS Publications website at DOI: 10.1021/acs.jpclett.6b02400.

Methodology details of the tDMRG simulation and DOS calculation as well as computational results for effects of system size and diagonal vibronic coupling on long-range charge separation in OSCs and Redfield simulations (PDF)

■ AUTHOR INFORMATION

Corresponding Author

*E-mail: haibo@nju.edu.cn.

ORCID

Haibo Ma: 0000-0001-7915-3429

Notes

The authors declare no competing financial interest.

■ ACKNOWLEDGMENTS

The work was supported by the National Natural Science Foundation of China (Grant Nos. 91333202, 11574052, 21373109), the National Basic Research Program of China (Grant No. 2012CB921401), and State Grid Corporation of China [2014]-1192. We are grateful to Profs. Alessandro Troisi, Yi Zhao, Zhenggang Lan, and Wenchao Yang for helpful discussions.

■ REFERENCES

- (1) Guo, J.; Ohkita, H.; Bente, H.; Ito, S. Charge Generation and Recombination Dynamics in Poly(3-hexylthiophene)/Fullerene Blend Films with Different Regioregularities and Morphologies. *J. Am. Chem. Soc.* **2010**, *132*, 6154–6164.
- (2) Bakulin, A. A.; Rao, A.; Pavelyev, V. G.; van Loosdrecht, P. H. M.; Pshenichnikov, M. S.; Niedzialek, D.; Cornil, J.; Beljonne, D.; Friend, R. H. The Role of Driving Energy and Delocalized States for Charge Separation in Organic Semiconductors. *Science* **2012**, *335*, 1340–1344.
- (3) Kaake, L. G.; Jasieniak, J. J.; Bakus, R. C., II; Welch, G. C.; Moses, D.; Bazan, G. C.; Heeger, A. J. Photoinduced Charge Generation in a Molecular Bulk Heterojunction Material. *J. Am. Chem. Soc.* **2012**, *134*, 19828–19838.
- (4) Grancini, G.; Maiuri, M.; Fazzi, D.; Petrozza, A.; Egelhaaf, H.-J.; Brida, D.; Cerullo, G.; Lanzani, G. Hot exciton dissociation in polymer solar cells. *Nat. Mater.* **2013**, *12*, 29–33.
- (5) Gélinas, S.; Rao, A.; Kumar, A.; Smith, S. L.; Chin, A. W.; Clark, J.; van der Poll, T. S.; Bazan, G. C.; Friend, R. H. Ultrafast Long-Range Charge Separation in Organic Semiconductor Photovoltaic Diodes. *Science* **2014**, *343*, 512–516.
- (6) Falke, S. M.; Rozzi, C. A.; Brida, D.; Maiuri, M.; Amato, M.; Sommer, E.; De Sio, A.; Rubio, A.; Cerullo, G.; Molinari, E.; Lienau, C. Coherent ultrafast charge transfer in an organic photovoltaic blend. *Science* **2014**, *344*, 1001–1005.
- (7) Provencher, F.; Bérubé, N.; Parker, A. W.; Greetham, G. M.; Towrie, M.; Hellmann, C.; Côté, M.; Stingelin, N.; Silva, C.; Hayes, S. C. Direct observation of ultrafast long-range charge separation at polymer/fullerene heterojunctions. *Nat. Commun.* **2014**, *5*, 4288.
- (8) Kaake, L. G.; Zhong, C.; Love, J. A.; Nagao, I.; Bazan, G. C.; Nguyen, T.-Q.; Huang, F.; Cao, Y.; Moses, D.; Heeger, A. J. Ultrafast Charge Generation in an Organic Bilayer Film. *J. Phys. Chem. Lett.* **2014**, *5*, 2000–2006.
- (9) Zhong, C.; Choi, H.; Kim, J. Y.; Woo, H. Y.; Nguyen, T. Q.; Huang, F.; Cao, Y.; Heeger, A. Ultrafast Charge Transfer in Operating Bulk Heterojunction Solar Cells. *Adv. Mater.* **2015**, *27*, 2036–2041.
- (10) Lee, J.; Vandewal, K.; Yost, S. R.; Bahlke, M. E.; Goris, L.; Baldo, M. A.; Manca, J. V.; Van Voorhis, T. Charge Transfer State Versus Hot Exciton Dissociation in Polymer-Fullerene Blended Solar Cells. *J. Am. Chem. Soc.* **2010**, *132*, 11878–11880.
- (11) Gregg, B. A. Entropy of Charge Separation in Organic Photovoltaic Cells: The Benefit of Higher Dimensionality. *J. Phys. Chem. Lett.* **2011**, *2*, 3013–3015.
- (12) Caruso, D.; Troisi, A. Long Range Exciton Dissociation in Organic Solar Cells. *Proc. Natl. Acad. Sci. U. S. A.* **2012**, *109*, 13498–13502.
- (13) Jailaubekov, A. E.; Willard, A. P.; Tritsch, J. R.; Chan, W.-L.; Sai, N.; Gearba, R.; Kaake, L. G.; Williams, K. J.; Leung, K.; Rossky, P. J.; Zhu, X.-Y. Hot charge-transfer excitons set the time limit for charge separation at donor/acceptor interfaces in organic photovoltaics. *Nat. Mater.* **2013**, *12*, 66–73.
- (14) Ma, H.; Troisi, A. Direct Optical Generation of Long-Range Charge-Transfer States in Organic Photovoltaics. *Adv. Mater.* **2014**, *26*, 6163–6167.
- (15) Savoie, B. M.; Jackson, N. E.; Chen, L. X.; Marks, T. J.; Ratner, M. A. Mesoscopic Features of Charge Generation in Organic Semiconductors. *Acc. Chem. Res.* **2014**, *47*, 3385–3394.
- (16) Vandewal, K.; Albrecht, S.; Hoke, E. T.; Graham, K. R.; Widmer, J.; Douglas, J. D.; Schubert, M.; Mateker, W. R.; Bloking, J. T.; Burkhard, G. F.; Sellinger, A.; Fréchet, J. M. J.; Amassian, A.; Riede, M. K.; McGehee, M. D.; Neher, D.; Salbeck, A. Efficient charge generation by relaxed charge-transfer states at organic interfaces. *Nat. Mater.* **2014**, *13*, 63–68.
- (17) Han, L.; Zhong, X.; Liang, W.; Zhao, Y. Energy relaxation and separation of a hot electron-hole pair in organic aggregates from a time-dependent wavepacket diffusion method. *J. Chem. Phys.* **2014**, *140*, 214107.
- (18) Gao, F.; Tress, W.; Wang, J.; Inganäs, O. Temperature Dependence of Charge Carrier Generation in Organic Photovoltaics. *Phys. Rev. Lett.* **2015**, *114*, 128701.
- (19) Monahan, N. R.; Williams, K. W.; Kumar, B.; Nuckolls, C.; Zhu, X.-Y. Direct Observation of Entropy-Driven Electron-Hole Pair Separation at an Organic Semiconductor Interface. *Phys. Rev. Lett.* **2015**, *114*, 247003.
- (20) Yao, Y. Spin-boson theory for charge photogeneration in organic molecules: Role of quantum coherence. *Phys. Rev. B: Condens. Matter Mater. Phys.* **2015**, *91*, 045421.
- (21) Devizis, A.; De Jonghe-Risse, J.; Hany, R.; Nüesch, F.; Jenatsch, S.; Gulbinas, V.; Moser, J.-E. Dissociation of Charge Transfer States and Carrier Separation in Bilayer Organic Solar Cells: A Time-Resolved Electroabsorption Spectroscopy Study. *J. Am. Chem. Soc.* **2015**, *137*, 8192–8198.
- (22) Few, S.; Frost, J. M.; Nelson, J. Models of charge pair generation in organic solar cells. *Phys. Chem. Phys.* **2015**, *17*, 2311–2325.
- (23) Grancini, G.; Binda, M.; Neutzner, S.; Criante, L.; Sala, V.; Tagliaferri, A.; Lanzani, G. The Role of Higher Lying Electronic States in Charge Photogeneration in Organic Solar Cells. *Adv. Funct. Mater.* **2015**, *25*, 6893–6899.
- (24) Gautam, B. R.; Younts, R.; Li, W.; Yan, L.; Danilov, E.; Klump, E.; Constantinou, I.; So, F.; You, W.; Ade, H.; Gundogdu, K. Charge Photogeneration in Organic Photovoltaics: Role of Hot versus Cold Charge-Transfer Excitons. *Adv. Energy Mater.* **2016**, *6*, 1501032.
- (25) Fazzi, D.; Barbatti, M.; Thiel, W. Unveiling the Role of Hot Charge-Transfer States in Molecular Aggregates via Nonadiabatic Dynamics. *J. Am. Chem. Soc.* **2016**, *138*, 4502–4511.
- (26) Pelzer, K. M.; Darling, S. B. Charge generation in organic photovoltaics: a review of theory and computation. *Mol. Syst. Des. Eng.* **2016**, *1*, 10–24.
- (27) D'Avino, G.; Muccioli, L.; Olivier, Y.; Beljonne, D. Charge Separation and Recombination at Polymer/Fullerene Heterojunctions: Delocalization and Hybridization Effects. *J. Phys. Chem. Lett.* **2016**, *7*, 536–540.

(28) Tamura, H.; Burghardt, I. Ultrafast Charge Separation in Organic Photovoltaics Enhanced by Charge Delocalization and Vibronically Hot Exciton Dissociation. *J. Am. Chem. Soc.* **2013**, *135*, 16364–16367.

(29) Heitzer, H. M.; Savoie, B. M.; Marks, T. J.; Ratner, M. A. Organic Photovoltaics: Elucidating the Ultra-Fast Exciton Dissociation Mechanism in Disordered Materials. *Angew. Chem., Int. Ed.* **2014**, *53*, 7456–7460.

(30) Bittner, E. R.; Silva, C. Noise-induced quantum coherence drives photo-carrier generation dynamics at polymeric semiconductor heterojunctions. *Nat. Commun.* **2014**, *5*, 3119.

(31) Smith, S. L.; Chin, A. W. Ultrafast charge separation and nongeminate electron-hole recombination in organic photovoltaics. *Phys. Chem. Chem. Phys.* **2014**, *16*, 20305–20309.

(32) Smith, S. L.; Chin, A. W. Phonon-assisted ultrafast charge separation in the PCBM band structure. *Phys. Rev. B: Condens. Matter Mater. Phys.* **2015**, *91*, 201302.

(33) Lee, M. H.; Aragó, J.; Troisi, A. Charge Dynamics in Organic Photovoltaic Materials: In-terplay between Quantum Diffusion and Quantum Relaxation. *J. Phys. Chem. C* **2015**, *119*, 14989–14998.

(34) Yao, Y.; Yang, W.; Zhao, Y. Exciton dissociation in the presence of phonons: A reduced hierarchy equations of motion approach. *J. Chem. Phys.* **2014**, *140*, 104113.

(35) Troisi, A. How quasi-free holes and electrons are generated in organic photovoltaic interfaces. *Faraday Discuss.* **2013**, *163*, 377–392.

(36) Vázquez, H.; Troisi, A. Calculation of rates of exciton dissociation into hot charge-transfer states in model organic photovoltaic interfaces. *Phys. Rev. B: Condens. Matter Mater. Phys.* **2013**, *88*, 205304.

(37) Ma, H.; Troisi, A. Modulating the Exciton Dissociation Rate Up to More Than 2 Orders of Magnitude by Controlling the Alignment of LUMO+1 in Organic Photovoltaics. *J. Phys. Chem. C* **2014**, *118*, 27272–27280.

(38) Brigeman, A. N.; Fusella, M. A.; Yan, Y.; Purdum, G. E.; Loo, Y.; Rand, B. P.; Giebink, N. C. Revealing the Full Charge Transfer State Absorption Spectrum of Organic Solar Cells. *Adv. Energy Mater.* **2016**, *6*, 1601001.

(39) Chin, A. W.; Rivas, A.; Huelga, S. F.; Plenio, M. B. Exact mapping between system-reservoir quantum models and semi-infinite discrete chains using orthogonal polynomials. *J. Math. Phys.* **2010**, *51*, 092109.

(40) Prior, J.; Chin, A. W.; Huelga, S. F.; Plenio, M. B. Efficient simulation of strong system-environment interactions. *Phys. Rev. Lett.* **2010**, *105*, 050404.

(41) Yao, Y.; Duan, L.; Lu, Z.; Wu, C. Q.; Zhao, Y. Dynamics of the sub-Ohmic spin-boson model: A comparison of three numerical approaches. *Phys. Rev. E* **2013**, *88*, 023303.

(42) Yao, Y.; Zhou, N.; Prior, J.; Zhao, Y. Competition between diagonal and off-diagonal coupling gives rise to charge-transfer states in polymeric solar cells. *Sci. Rep.* **2015**, *5*, 14555.

(43) The number of LRCT microstates Ω is approximately proportional to the number of donor molecules (N_D) multiplied by the number of acceptor molecules (N_A). As both N_D and N_A scale as L^D , where L is the system width and D is the system dimensionality, Ω is proportional to L^{2D} , and, accordingly, entropy $S = k \ln \Omega$ is proportional to dimensionality D .

(44) Hood, S. N.; Kassal, I. Entropy and disorder enable charge separation in organic solar cells. *J. Phys. Chem. Lett.* **2016**, *7*, 4495–4500.